J Korean Soc Appl Biol Chem (2015) 58(5):751–760
DOI 10.1007/s13765-015-0103-1

Online ISSN 2234-344X
Print ISSN 1738-2203

ARTICLE

Characteristics of biochars derived from fruit tree pruning wastes and their effects on lead adsorption

Jong Hwan Park[1] · Yong Sik Ok[2] · Seong Heon Kim[1] · Se Won Kang[4] · Ju Sik Cho[4] · Jong Soo Heo[1] · Ronald D. Delaune[3] · Dong Cheol Seo[4]

Received: 25 February 2015 / Accepted: 13 July 2015 / Published online: 25 July 2015

Abstract The aim of this study was to evaluate the biochar characteristics derived from fruit tree pruning wastes (FTPW) and their effects on lead (Pb) adsorption. Based on results from Pb adsorption, surface area, and phosphorus content, the optimum pyrolysis temperature was 600 °C for Pb adsorption capacity. Using the Freundlich isotherm, the Pb adsorption capacity (K) of biochar obtained from various FTPW decreased in the order of pear (3.8001) ≫ persimmon (2.3977) ≥ apple (2.1968). Based on the Langmuir adsorption isotherm, the maximum Pb adsorption capacities (a; mg g^{-1}) of biochar obtained from different FTPW were in the following order: pear (26.2) ≫ persimmon (19.9) ≥ apple (17.7). The maximum Pb adsorption capacity of the pruned pear tree waste biochar was greater than the other FTPW biochars. Pruned apple tree waste biochar had the lowest Pb adsorption capacity among the tested FTPW biochars. The positive correlation between the Langmuir maximum adsorption capacity (L_M) values of the biochars and their phosphorus content and surface area indicated difference in adsorption capacity. However, adsorption capacity of the biochar from all FTPW studied could be used for removing Pb and other metal from wastewater.

Keywords Biochar · Freundlich isotherm · Fruit tree pruning waste · Langmuir isotherm · Lead adsorption

✉ Ju Sik Cho
chojs@sunchon.ac.kr

✉ Dong Cheol Seo
drseodc@gmail.com

[1] Divison of Applied Life Science (BK21 Plus) & Institute of Agriculture and Life Science, Gyeongsang National University, Jinju 660-701, Republic of Korea

[2] Korea Biochar Research Center & Department of Biological Environment, Kangwon National University, Chuncheon 200-701, Republic of Korea

[3] Department of Oceanography and Costal Sciences, School of the Coast and Environment, Louisiana State University, Baton Rouge, LA 70803, USA

[4] Department of Bio-Environmental Sciences, Sunchon National University, Suncheon 540-950, Republic of Korea

Introduction

In 2012, the surface area occupied by sweet fruit trees in Korea was nearly a 150,000 ha, corresponding to the following main crops pear tree (17,090 ha), apple tree (30,451 ha), and persimmon tree (30,347 ha). Production of fruit tree pruning waste (FTPW) was 63,478 tons per year (KREI 2014). Pruning wastes from fruit tree branches are characterized by low-middle moisture and high cellulose and lignin contents. After being collected, most of these wastes are normally burnt for removal. An alternative is land disposal of fragmented woody debris for nutrient recycling which is being slowly implemented in South Korea. However, these in practices can create environmental pollution problems and limited value to the industry (Hameed et al. 2008). Therefore, in recent years, many researchers have tried recycling FTPW by creating products (Demirbas et al. 2008; Hameed et al. 2008; Tan et al. 2008; Abdulrazzaq et al. 2014).

Biochar is a carbon-rich by-product synthesized through pyrolysis/carbonization of biomass such as wood, manure, food waste, organic by-products, bioenergy crops, crop residues, forestry waste, sewage sludge, or any other organic material (Ahmad et al. 2012; Houben et al. 2013; Waqas et al. 2015). An increasing interest in the beneficial

application of biochar has opened up multi-disciplinary areas for science and engineering. The potential biochar applications include carbon sequestration, soil fertility improvement, pollution remediation, and agricultural by-product/waste recycling (Khan et al. 2013, 2014; Smider and Singh 2014; Waqas et al. 2015).

Water contamination with heavy metals such as Pb^{2+} discharged from industrial effluents has become a worldwide problem during recent years. These heavy metals have toxic effects on all living organisms and continuously accumulate in biota and their food chain (Lu et al. 2012). Thus, wastewater containing Pb^{2+} needs to be purified and recycled in order to secure alternative sources of water (Ali 2010).

According to Gupta et al. (2009), among various treatment technologies, adsorption is a fast and universal method for treating heavy metals with great efficiency and low expense. Various sorbents (natural materials and synthetic products) have been developed. Recently, several studies have suggested that biochar can be an effective material for the sorption of heavy metals from wastewater (including aqueous solution) as well as an amendment for immobilization of heavy metals in contaminated soils (Chen et al. 2011; Inyang et al. 2012; Xu et al. 2013). Use of biochar as a sorbent for treating wastewater containing heavy metals is an emerging and promising treatment technology (Ahmad et al. 2014). Biochars derived from plant residues and agricultural wastes have been tested for their abilities to sorb various heavy metals (Pb, Cu, Ni, and Cd) (Uchimiya et al. 2010, 2011). However, there is very limited knowledge of the effects of various biochars on metal adsorption processes (Chen et al. 2011). Especially, detailed investigation is needed to understand the mechanism or effectiveness of FTPW biochar for Pb removal.

The aim of this study was to evaluate the interaction between various FTPW biochar characteristics as related to Pb adsorption. The specific objectives were (i) to analyze FTPW-derived biochar characteristics (with SEM–EDS and FTIR), (ii) to compare the adsorption capacities of Pb adsorption isotherms using both Freundlich and Langmuir adsorption models, and (iii) to investigate the interaction between FTPW biochar characteristics and Pb adsorption.

Materials and methods

Material

Fruit tree pruning wastes were collected from a local agricultural field (pear, 35°17′41.92″N latitude and 128°16′28.23″E longitude in Munsan-eup, Jinju-si; apple, 35°56′62.72″N latitude and 128°92′90.98″E longitude in Sinwon-myeon, Geochang-gun; persimmon, 35°01′03.06″N latitude and 128°9′53.43″E longitude in Yonghyeon-myeon, Sacheon-si) in Korea. Each FTPW was rinsed three times with distilled water, dried in an oven at 110 °C until constant weight, cut and sieved for a particle size of 1–2 mm.

Biochar production using fruit tree branches

A slow pyrolyzer was used to convert the samples into biochars. The raw feedstock was placed in a stainless airtight container with a cover and pyrolyzed in a furnace (DK-1015(E), STI tech, Korea) under a limited oxygen condition. The airtight container was purged with nitrogen gas (10 psi), and oxygen content of the airtight container was less than 0.5 % before being inserted into the furnace. The controller of the furnace was programmed to drive the internal biomass chamber temperature to 600 °C at a rate of 10 °C min^{-1}, after which the peak temperature was held for 4 h before cooling to room temperature. Biochar produced by pyrolysis was gently crushed and sieved to <0.5 mm. In addition, the FTPW biochar samples were washed with DI water three times to remove impurities (e.g., ash) and soluble salts before adsorption experiment. The pH values of the FTPW biochars after washing were slightly lower than those in raw biochars without washing. Decreasing pH values are mainly due to washing of soluble salts from raw biochars (data not shown). The biochar samples were then oven-dried (80 °C), and sealed in an airtight container before use.

Characterization of biochar

The pH of FTPW biochar was measured using a pH meter (Orion, Thermo Electron Corp., USA) in a 1 % (W V^{-1}) suspension in DI water prepared by shaking at 100 rpm for 2 h. BET (Brunauer–Emmett–Teller) surface areas of FTPW biochar were measured via N_2 adsorption multilayer theory using an ASAP-2020 M analyzer (Micromeritics Instrument Corp., USA). The FTPW biochar samples were degassed for 6 h under vacuum conditions at 473 K before adsorption measurement. The data were fitted to the BET equation in order to calculate the surface area. Total pore volume was estimated from N_2 adsorption at $P/P_o \sim 0.5$. The Barret–Joyner–Halender method was used to determine the pore-size distribution from the N_2 desorption isotherms (Ahmad et al. 2012). The elemental composition (C, H, N, S, and O) of FTPW-derived biochar was determined by dry combustion using an elemental analyzer (LECO TruSpec CHN, USA). The data were used to calculate molar ratios of H/C, O/C, (O + N)/C, and (O + N + S)/C in order to evaluate relationships between the pyrolysis temperature and the relative degree of hydrophobicity of biochar.

The mineralogy of the FTPW biochars phases were analyzed using a Personal SEM (Philips XL 30S FEG,

Netherlands) equipped with backscattered and secondary electron detectors coupled with EDS. The SEM–EDS provided detailed imaging information about the morphology and surface texture of individual particles, as well as the elemental composition of the FTPW biochar samples.

The spectral properties of FTPW biochars were examined by Fourier transform infrared spectroscopy (FTIR) (Bruker VERTEX 70, BRUKER OPTICS, Germany). FTIR spectra were obtained at 2 cm^{-1} resolution from 400 to 4000 cm^{-1} using a combined 128 scans. The FTIR spectral peak assignments were interpreted based on characteristic vibrations for soybean stover- and peanut shell-derived biochars (Ahmad et al. 2012) as well as plant biomass-derived biochars (Keiluweit et al. 2010).

Batch experiment

Batch experiments were conducted to determine the adsorption characteristics of various FTPW biochars for the Pb. Adsorption behaviors of the Pb by FTPW biochars were evaluated using both the Freundlich and Langmuir adsorption isotherm equations. Stock solution (1000 mg L^{-1}) of Pb ($Pb(NO_3)_2$) was prepared by dissolving exact quantities of respective salts (GR grade, Fisher Scientific, USA) in double-distilled water. The stock solution was further diluted to the required experimental concentration.

Adsorption isotherms of Pb were obtained by weighing 0.1 g of FTPW biochars (600 °C, 4 h) from each test in glass Erlenmeyer flasks. Thereafter, 50 mL of solution containing specific concentrations of the metals was added to the flask. For Pb, concentration levels of 0, 2.5, 5, 10, 20, 40, 80, 160, and 320 mg L^{-1} were individually evaluated. The initial pH of the solutions were adjusted to 6 by adding either 0.1 M HCl or 0.1 M NaOH solutions. After providing sufficient time for the system to reach equilibrium, all samples were equilibrated for 24 h on a rotary shaker (KASI KSI-200L, Korea) at constant room temperature (25 °C). After settling, a 30-mL aliquot of the supernatant was filtered through a Whatman GF/C filter (0.45 μm) and then analyzed for metal concentrations. The concentrations of Pb in the adsorption experiments were determined using inductively coupled plasma with optical emission spectroscopy (ICP–OES, Perkin Elmer Optima 4300 DV). The amount of metal adsorption by FTPW biochars was calculated from the concentration reduction in solution.

Adsorption models

Adsorption isotherms were determined using the Freundlich and Langmuir models. The Freundlich isotherm is more widely used and deals with heterogeneous surface adsorption. The Freundlich equation (Bohn et al. 1979) in its original form (1) can be written as

$$q = KC_e^{\frac{1}{n}}, \quad (1)$$

where q (mg kg^{-1}) is the species concentration in the sorbent material (adsorption capacity), K is a constant related to the adsorption capacity, C_e (mg L^{-1}) is the concentration in solution, and n is an empirical parameter related to the intensity of adsorption, which varies with the heterogeneity of the material.

The most widely used isotherm equation for modeling the equilibrium is the Langmuir equation, which is valid for monolayer sorption onto a surface with a finite number of identical sites. The Langmuir equation (Bohn et al. 1979) in its original form (2) can be written as

$$q = \frac{abC_e}{1 + bC_e}, \quad (2)$$

where C_e (mg L^{-1}) is the concentration of heavy metal in solution at equilibrium, q (mg kg^{-1}) is the mass of heavy metal adsorbed to the biochar, a (mg kg^{-1}) is the maximum adsorption capacity of heavy metal, and b is a constant related to the binding strength of heavy metal, which represents the inverse of the equilibrium concentration of adsorption at one-half saturation.

Statistical analysis

Statistical analysis of data was conducted using SAS software (SAS 9.3, SAS Institute Inc. USA). Simple linear regression using PROC REG (SPSS 21, SPSS Institute Inc. USA) was conducted in order to determine if the slope of a regression was significantly different from the theoretical model ($\alpha = 0.05$). The relationships between parameters were determined using Pearson's correlation coefficients (r).

Results and Discussion

Characterization of biochar

Physico-chemical properties of FTPW biochars were analyzed, and the results are shown in Table 1. The pH of FTPW biochars increased as pyrolysis temperature increased, suggesting that higher pyrolysis temperature led to the higher pH of the biochars. Novak et al. (2009) obtained a similar result, showing that biochars produced from poultry litter had the highest pH values of between 8.7 and 10.3. Yuan et al. (2011) reported that these increases in pH values are mainly due to separating of alkali salts from organic materials by increased pyrolysis temperature.

Table 1 Physico-chemical characteristics of fruit tree pruning waste biochars under different pyrolysis temperatures

Content	Temperature (°C)	pH (1:25)	C (%)	H (%)	N (%)	S (%)	O (%)	T-P (%)	H/C	O/C	(O + N)/C	(O + N + S)/C	Yield (%)	SA (m^2 g^{-1})
Pear	300	8.94	66.68	5.65	2.91	0.14	24.62	1.15	1.02	0.28	0.314	0.315	34.5	1.5
	400	9.29	69.58	4.73	3.21	0.11	22.63	1.40	0.82	0.24	0.280	0.281	26.4	3.6
	500	9.32	73.45	3.73	2.98	0.10	19.74	1.72	0.61	0.20	0.236	0.237	22.7	22.7
	600	10.08	75.09	3.52	2.95	0.10	18.34	2.00	0.56	0.18	0.217	0.217	20.3	134.2
Apple	300	8.51	67.34	5.70	2.98	0.27	23.71	0.74	1.02	0.26	0.302	0.304	36.5	2.2
	400	9.58	70.05	5.09	3.18	0.17	21.51	1.06	0.87	0.23	0.269	0.270	26.7	3.1
	500	9.82	77.16	4.02	2.71	0.13	15.98	1.37	0.63	0.16	0.185	0.186	23.6	13.6
	600	10.27	79.26	3.14	2.59	0.12	14.89	1.49	0.48	0.14	0.169	0.169	22.5	99.4
Persimmon	300	8.12	67.63	5.51	2.75	0.15	23.96	0.77	0.98	0.27	0.300	0.301	37.9	1.7
	400	9.55	71.12	4.66	3.06	0.20	20.96	1.13	0.79	0.22	0.258	0.259	29.2	2.9
	500	9.71	72.28	3.82	2.96	0.31	20.63	1.45	0.63	0.21	0.249	0.250	25.5	17.4
	600	9.89	76.87	2.85	2.71	0.18	17.39	1.63	0.45	0.17	0.200	0.201	22.3	114.1

H/C atomic ratio of hydrogen to carbon, *O/C* atomic ratio of oxygen to carbon, *(O + N)/C* atomic ratio of sum of nitrogen and oxygen to carbon, *(O + N + S)/C* atomic ratio of sum of nitrogen, oxygen and sulfur to carbon, *SA* BET-N_2 specific surface area

The yields of biochar under different FTPW and pyrolysis temperature were 34.5 % at 300 °C, 26.4 % at 400 °C, 22.7 % at 500 °C, and 20.3 % at 600 °C in pear tree pruning waste biochar, 36.5 % at 300 °C, 26.7 % at 400 °C, 23.6 % at 500 °C, and 22.5 % at 600 °C in apple tree pruning waste biochar, and 37.9 % at 300 °C, 29.2 % at 400 °C, 25.5 % at 500 °C, and 22.3 % at 600 °C in persimmon tree pruning waste biochar showing that FTPW biochar yield decreased with pyrolysis temperature increasing. Ahmad et al. (2012) obtained a similar result, showing that yield of soybean stover- and peanut shell-derived biochars decreased from 37 to 22 % as temperature increased from 300 to 700 °C. Uchimiya et al. (2011) converted cottonseed hulls into biochar at various pyrolysis temperatures ranging from 200 to 800 °C. A rapid decrease in biochar yield was observed at 400 °C due to the loss of volatile matter and non-condensable gases (CO_2, CO, H_2, and CH_4), whereas at >400 °C, a steady biochar yield was observed. The biochar yield at >400 °C was fairly consistent because of the low lignin content in cottonseed hulls. A comprehensive comparison was made by Keiluweit et al. (2010) among different biochars derived from grass and wood biomass based on pyrolysis temperature. A rapid decline in biochar yield at <300 °C was reported due to initial dehydration reactions. Relatively lower lignin contents in grass compared to wood caused an earlier thermal breakdown at low pyrolysis temperatures (200–400 °C).

In this study, the surface area of FTPW biochar increased as pyrolysis temperature increased. Especially, when surface area of FTPW biochar increased from 1.5 to 134 m^2 g^{-1} as temperature increased from 300 to 600 °C. Especially, pear tree pruning waste biochar had higher surface area than the other FTPW biochars, whereas apple tree pruning waste biochar had the lowest surface area among the tested FTPW biochars. Ahmad et al. (2014) reported that surface area increases with increases in pyrolysis temperature. However, according to Uchimiya et al. (2011), a reduction in surface area at above 700 °C has been reported.

The C and T-P contents (%) were increased, whereas O and H contents (%) were decreased with pyrolysis temperature increasing. Total nitrogen content of FTPW biochar decreased by 7−18 % when the temperature was increased 600 °C compared to 400 °C. This may be due to the volatilization of nitrogen during pyrolysis (Bagreev et al. 2001; Gaskin et al. 2008). Shinogi (2004) also reported a decrease of total N in the biochar produced from sewage sludge at higher temperatures. Nitrogen is removed through loss of the NH_4–N and NO_3–N fraction as well as the loss of volatile matter containing N groups at temperature of 200 °C, but with increased temperature (>600 °C) it is gradually transformed into pyridine-like structure (Bagreev et al. 2001).

The molar H/C, O/C, (O + N)/C, and (O + N + S)/C) ratios were decreased with pyrolysis temperature increasing, indicating biochar was highly carbonized and exhibited higher aromaticity at 600 °C in comparison with 300 °C, as reported by Chen et al. (2008). Ahmad et al. (2012) reported lower molar ratios for various biochars produced at 600 °C, which is similar with our results.

A van Krevelen diagram (Fig. 1), constructed for FTPW biochars clearly demonstrates that a plant-based biomass undergoes dehydration and depolymerization into smaller dissociation products of lignin and cellulose with an increase in pyrolysis temperature (Keiluweit et al. 2010).

Chen et al. (2008) showed the decreasing H/C and O/C ratios related to a higher aromaticity and lower polarity of biochars derived from pine needles. These findings were further supported by Chen and Chen (2009) and Uchimiya et al. (2010).

SEM and EDS

Morphology and surface structural (Fig. 2) changes in FTPW biochar were also influenced by pyrolysis temperature. In general, surface area increases with an increase in pyrolysis temperature. However, a reduction in surface area at 700 °C has also been reported (Uchimiya et al. 2011). According to Chen and Chen (2009), destruction of aliphatic alkyl and ester groups, and exposure of the aromatic lignin core through higher pyrolysis temperatures may be responsible for an increase in surface area. A positive correlation between micropore volume and surface area suggests that the pore-size distribution is a key factor responsible for the increase in surface area in biochar (Downie et al. 2007).

The elemental composition of FTPW biochars at 300, 400, 500 and 600 °C were analyzed by Energy Dispersive Spectrometer (EDS). A rise in pyrolysis temperature increased C content, whereas H and O contents decreased (Figs. 3, 4), thereby indicating dehydration and deoxygenation of the biomass.

FTIR

The FTIR spectra for FTPW (pear, apple, and persimmon) biochar (pyrolysis temp. 300, 400, 500, and 600 °C) are shown in Fig. 5. Several peaks were observed in the three FTPW biochars. The FTIR spectra of biochars were similar (except for C–H stretching band) regardless of feedstock type.

For FTPW biochars obtained from pear, apple, and persimmon, the peaks were related to symmetric C–O stretching and aromatic C–H groups at 885 cm^{-1} (Keiluweit et al. 2010). The peak at 1440 cm^{-1} in all tested FTPW biochars indicated the presence of aromatic C=C stretching (Keiluweit et al. 2010). The peak observed at 1514 cm^{-1} in the FTPW biochar could be attributed to secondary aromatic amines (Das et al. 2009). The aromatic C=C stretching and C=O stretching of conjugated ketones and quinones (C=C and C=N functional groups) for FTPW biochars produced from pear, apple, and persimmon were identified in the band from 1595 to 1600 cm^{-1} (Keiluweit et al. 2010). The peaks at 1645–1653 cm^{-1} decreased in all tested FTPW biochars at 600 °C as compared to biochar at 300 °C which are related to C=O stretching vibrations for amides (Das et al. 2009).

The C–H stretching bands at 2930 cm^{-1} (asymmetric) and 2870 cm^{-1} (symmetric) were assigned to the $–CH_2$ and $–CH_3$ groups for the FTPW biochar produced from pear (except for apple and persimmon) for at 300 °C, respectively (Das et al. 2009; Keiluweit et al. 2010). The peaks at 2930 cm^{-1} (asymmetric) and 2870 cm^{-1} (symmetric) decreased in pear tree pruning waste biochar at 600 °C as compared to pear tree pruning waste biochar at 300 °C. Ahmad et al. (2012) reported that the peaks of the C–H stretching bands in soybean stover- and peanut shell-derived biochars decreased as pyrolysis temperature increased. Chen et al. (2008) also reported a reduction in polar functional groups with increasing carbonization temperature. The broad band near 3300 cm^{-1} for the FTPW biochars derived from pear, apple, and persimmon at 300 °C were attributed to the stretching vibration of hydrogen-bonded hydroxyl groups (Keiluweit et al. 2010), whereas it decreased as pyrolysis temperature increased. According to Cantrell et al. (2012), these changes can be attributed to the transformation products of lignin and cellulose. These results also agree with studies by Keiluweit et al. (2010), Ahmad et al. (2012), Chen et al. (2008), and Rajapaksha et al. (2014).

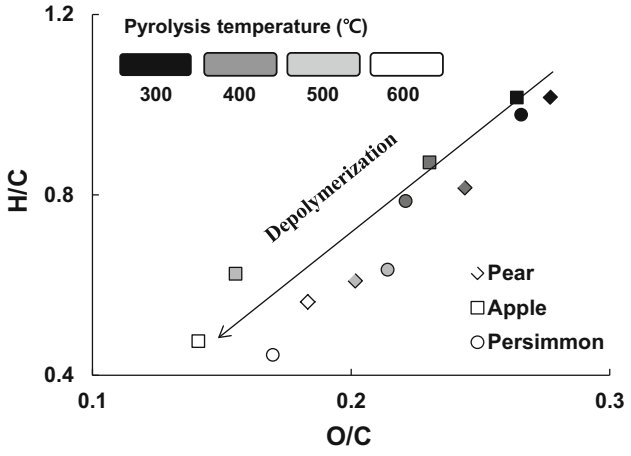

Fig. 1 van Krevelen diagram of fruit tree pruning waste biochars manufactured under different pyrolysis temperatures

Lead adsorption characteristics of various fruit tree pruning waste biochar

The Pb adsorption isotherms obtained by testing the FTPW biochars in the batch experiment are shown in Fig. 6A. The results showed the relationship between the equilibrium concentration (C_e) and the amount of adsorbed Pb in the supernatant solutions with filtration at the end of the adsorption experiment.

The Pb adsorption capacities of the FTPW biochar using Freundlich and Langmuir isotherms were expressed as

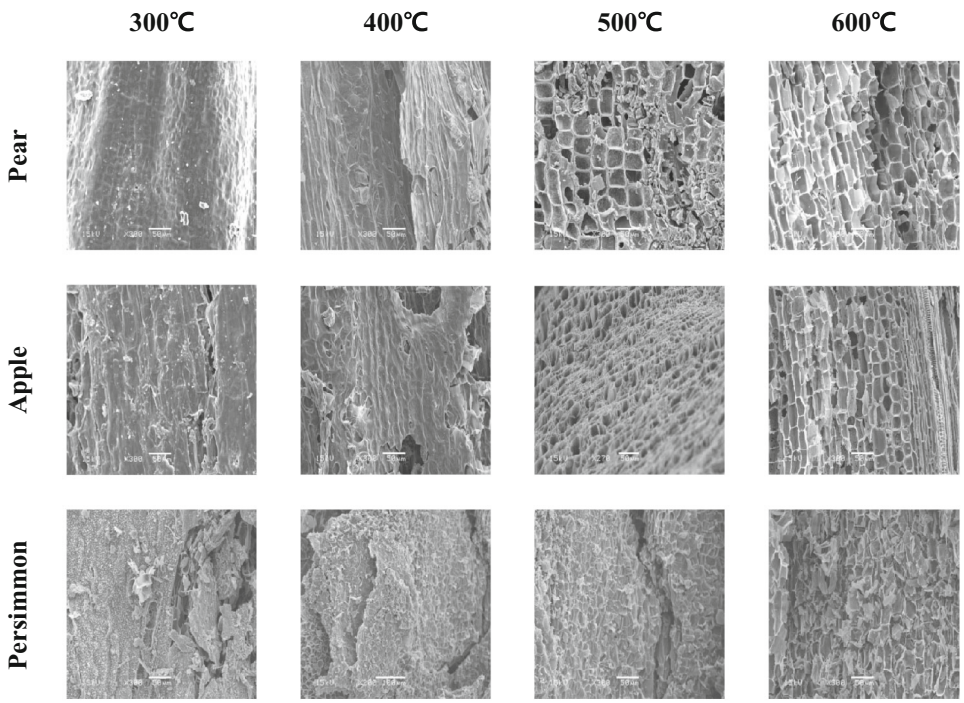

Fig. 2 SEM micrographs of fruit tree pruning waste biochar manufactured under different pyrolysis temperatures

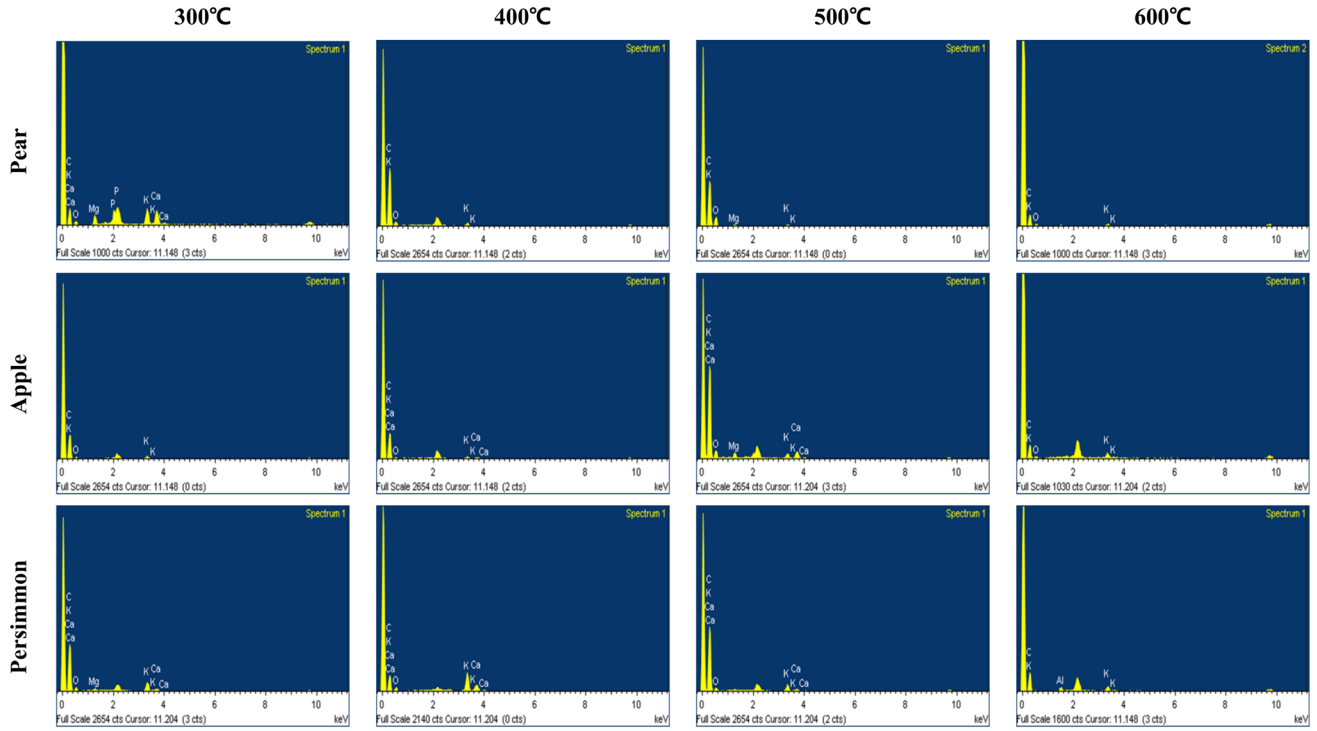

Fig. 3 EDS scans of fruit tree pruning waste biochar manufactured under different pyrolysis temperatures

linear regression. Using the Freundlich isotherm, the Pb adsorption capacity (K) of biochar obtained from different FTPW decreased in the order pear (3.8001) $\gg$ persimmon (2.3977) $\geq$ apple (2.1968) (Fig. 6B; Table 2). In this study, the values of $1/n$ in the adsorption isotherms for all tested FTPW biochars were less than unity, suggesting a favorable adsorption process. As indicated by the Freundlich K values, the pruned pear tree waste biochar had higher Pb adsorption capacity than the other FTPW biochar.

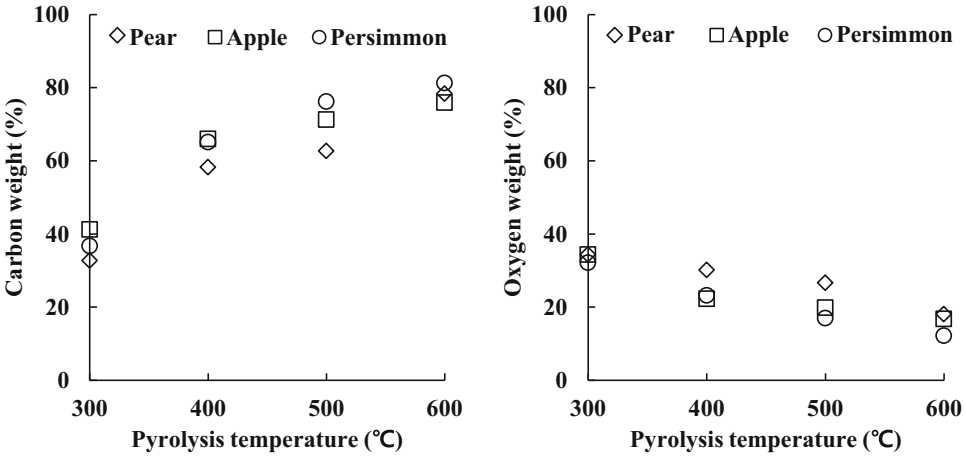

Fig. 4 Carbon and Oxygen weight obtained from EDS scan of fruit tree pruning waste biochar surface under different pyrolysis temperatures

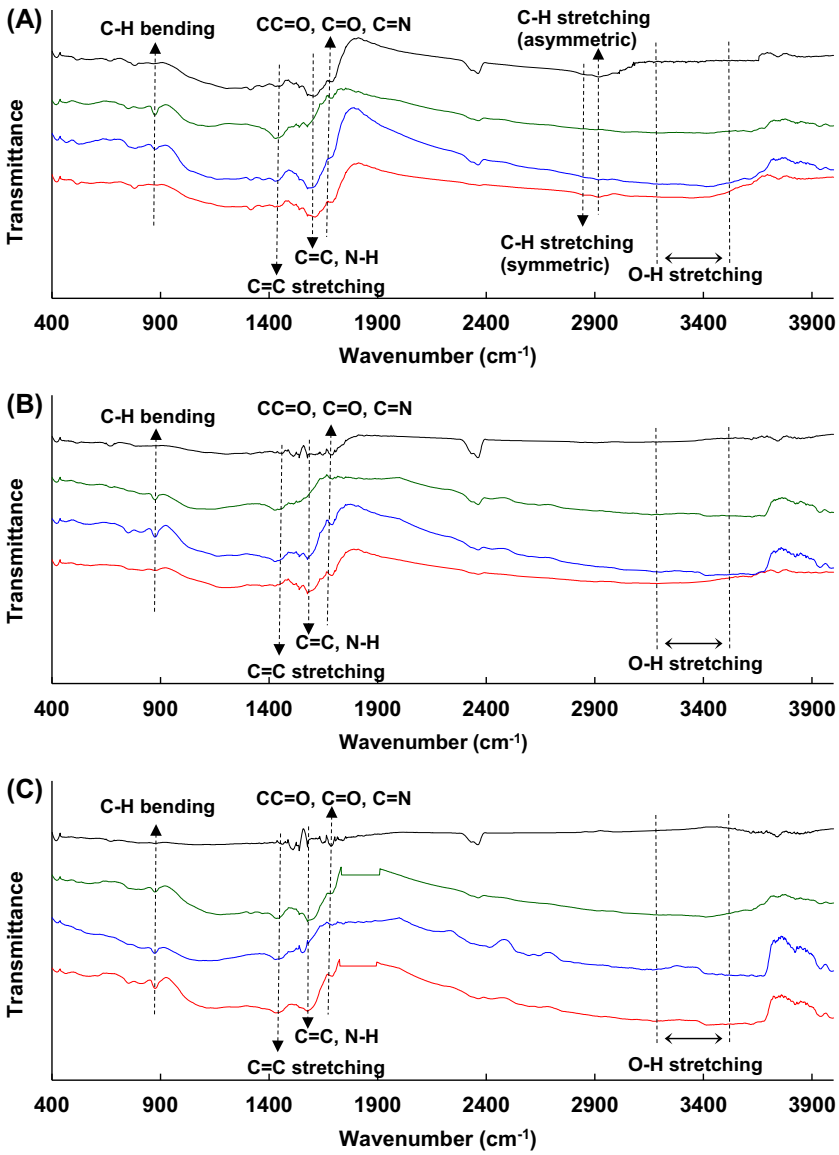

Fig. 5 Relative change in FTIR wave number identification of fruit tree pruning waste biochar manufactured under different pyrolysis temperatures. (**A**) pear; (**B**) apple; (**C**) persimmon; *red curve* 300 °C; *blue curve*, 400 °C; *green curve* 500 °C; *black curve* 600 °C

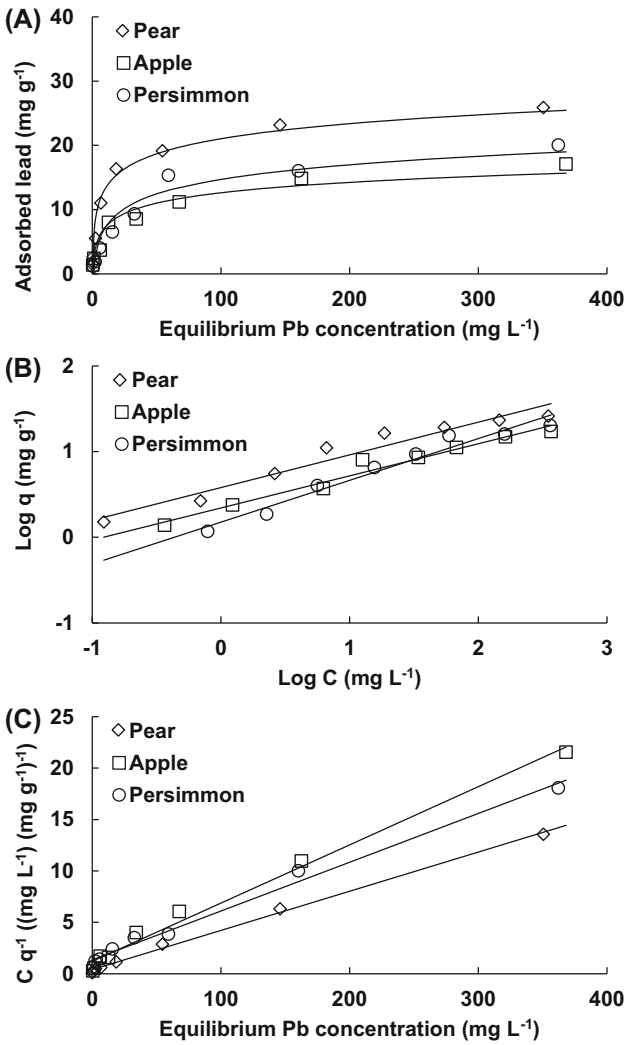

Fig. 6 Adsorption isotherms for the lead by fruit tree pruning waste-derived biochar. (**A**) Adsorption isotherm; (**B**) Freundlich isotherm; (**C**) Langmuir isotherm

Based on the Langmuir adsorption isotherm, the maximum Pb adsorption capacities (a; mg g^{-1}) of biochar obtained from different the FTPW were in the following order: pear (26.2) $\gg$ persimmon (19.9) $\geq$ apple (17.7) (Fig. 6C; Table 2). The maximum Pb adsorption capacities of the pruned pear tree waste were greater than the other FTPW biochars, whereas pruned apple tree waste biochar had the lowest Pb adsorption capacity among the tested FTPW biochars.

The binding strength constant (b) of Pb determined from the Langmuir isotherms in the FTPW biochars ranged from 0.0361 to 0.0977. The b value of Pb in FTPW biochars was in the order $b_{\text{pear}} \gg b_{\text{persimmon}} \geq b_{\text{apple}}$. Higher b values have been related to specific sorption of Pb on high energy surfaces with low dissociation constants. On the other hand, lower b values appear to be related to sorption on low energy surfaces with high dissociation constants (Adhikari and Singh 2003).

According to Uchimiya et al. (2010), mechanisms for heavy metal including Pb retention by biochars include the formation of metal hydroxide, oxide, carbonate, and phosphate precipitates and/or the activation of surfaces caused by the increase in pH. Another possible mechanism of heavy metal retention by biochars is specific metal–ligand complexation involving surface functional groups of chars with or without cation exchange (Uchimiya et al. 2010). Keiluweit et al. (2010) has suggested that adsorption mechanisms for heavy metals by biochar are based on sorptive interactions between the aromatic π-electrons of biochars and d-electrons of metals.

Interaction between biochar characteristics and Pb adsorption

The maximum adsorption capacity of Pb in FTPW biochars was in the order of pear $\gg$ persimmon $\geq$ apple. Higher Pb adsorption capacity of pear tree pruning waste biochar was not shown in significance in relation to the properties of biochar except T-P content and surface area. Thus, the results were described only for the correlation between the

Table 2 Determination of the parameters for the Freundlich and Langmuir adsorption isotherm by test fit approach in experiment of lead adsorption to fruit tree pruning waste-derived biochars

Fruit tree pruning waste biochar	Freundlich adsorption isotherm			Langmuir adsorption isotherm		
	Equation	K	$1/n$	Equation	a	b
Pear	$y = 0.3817x + 0.5798$ ($r = 0.984$**)	3.8001	0.3817	$y = 0.0381x + 0.3982$ ($r = 0.949$**)	26.2	0.0956
Apple	$y = 0.3748x + 0.3418$ ($r = 0.980$**)	2.1968	0.3748	$y = 0.0566x + 1.2086$ ($r = 0.955$**)	17.7	0.0468
Persimmon	$y = 0.3841x + 0.3798$ ($r = 0.979$**)	2.3977	0.3841	$y = 0.0502x + 1.1153$ ($r = 0.991$**)	19.9	0.0450

K adsorption capacity of Pb, $1/n$ an empirical parameter related to the intensity of sorption, a maximum adsorption capacities of Pb (mg g^{-1}), b binding strength constant of Pb

** Denote significance at 1.0 % levels

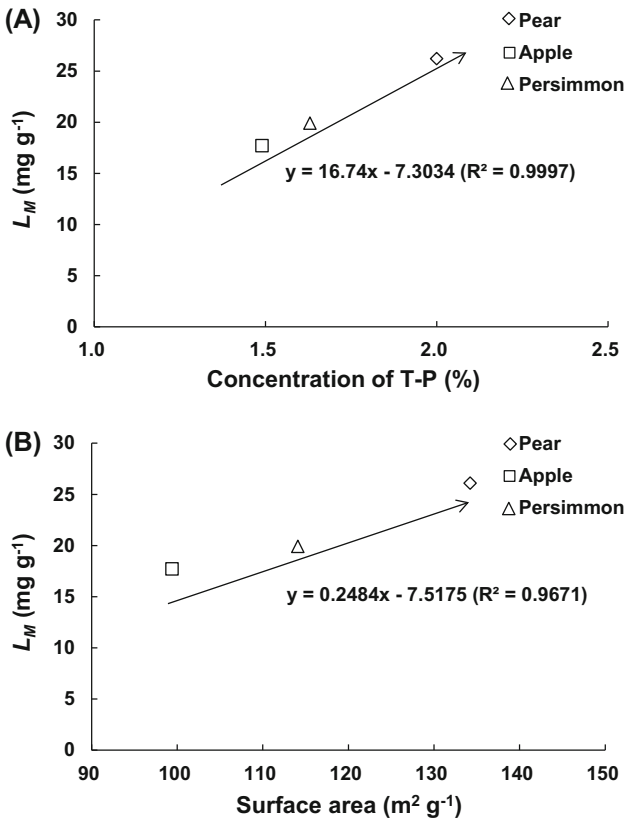

Fig. 7 Correlation among Langmuir adsorptive capacity (L_M) versus phosphorus content (**A**) and surface area (**B**) of various fruit tree pruning waste biochars

phosphorus content and surface area and the absorption properties of lead.

The Pb adsorption capacity of various FTPW biochar was correlated with their properties including T-P content and surface area (Fig. 7). The lead adsorption capacities (L_M) of biochar under different FTPW were taken from the Langmuir adsorption isotherms at a constant Pb equilibrium concentration. The L_M was positively correlated with T-P content. The highest T-P content occurred by pear tree pruning waste biochar. Phosphate induced Pb^{2+} immobilization soil has been extensively investigated where phosphate was shown to reduce Pb leachability via the formation of lead phosphate compounds such aspyromorphite-like phases ($Pb_5(PO_4)_3X$, X = F, Cl, OH) (Zhang and Ryan 1999; Cao et al. 2002; Scheckel and Ryan 2002).

The positive correlation between the L_M values of FTPW biochars and their surface area indicated their interdependence. A similar dependence of adsorption capacity on surface area has been reported by Chen et al. (2008) and Erto et al. (2010). The removal of volatile matter from biochars at high temperature would have resulted in the development of micropores causing increased surface area leading to greater diffusion of Pb into these micropores.

Acknowledgments This work was supported by the National Research Foundation of Korea grant funded by the Korea Government (Ministry of Education, Science and Technology), [NRF-2014R1A1A2007515].

References

Abdulrazzaq H, Jol H, Husni A, Abu-Bakr R (2014) Characterization and stabilization of biochars obtained from empty fruit bunch, wood, and rice husk. BioResource 9:2888–2898

Adhikari R, Singh MV (2003) Sorption characteristics of lead and cadmium in some soils of India. Geoderma 114:81–92

Ahmad M, Lee SS, Dou X, Mohan D, Sung JK, Yang JE, Ok YS (2012) Effects of pyrolysis temperature on soybean stover- and peanut shell-derived biochar properties and TCE adsorption in water. Bioresour Technol 118:536–544

Ahmad M, Rajapaksha AU, Lim JE, Zhang M, Bolan N, Mohan D, Vithanage M, Lee SS, Ok YS (2014) Biochar as a sorbent for contaminant management in soil and water: a review. Chemosphere 99:19–23

Ali I (2010) The quest for active carbon adsorbent substitutes: inexpensive adsorbents for toxic metal ions removal from wastewater. Sepn Purifn Rev 39:95–171

Bagreev A, Bandosz TJ, Locke DC (2001) Pore structure and surface chemistry of adsorbents obtained by pyrolysis of sewage derived fertilizer. Carbon 39:1971–1979

Bohn H, McNeal G, O'connor G (1979) Soil chemistry. Wiley, New York

Cantrell KB, Hunt PG, Uchimiya M, Novak JM, Ro KS (2012) Impact of pyrolysis temperature and manure source on physicochemical characteristics of biochar. Bioresour Technol 107:419–428

Cao X, Ma LQ, Chen M, Singh SP, Harris WG (2002) Impacts of phosphate amendments on lead biogeochemistry at a contaminated site. Environ Sci Technol 36:5296–5304

Chen B, Chen Z (2009) Sorption of naphthalene and 1-naphthol by biochars of orange peels with different pyrolytic temperatures. Chemosphere 76:127–133

Chen B, Zhou D, Zhu L (2008) Transitional adsorption and partition of nonpolar and polar aromatic contaminants by biochars of pine needles with different pyrolytic temperatures. Environ Sci Technol 42:5137–5143

Chen X, Chen G, Chen L, Chen Y, Lehmann J, McBride MB, Hay AG (2011) Adsorption of copper and zinc by biochars produced from pyrolysis of hardwood and corn straw in aqueous solution. Bioresour Technol 102:8877–8884

Das DD, Schnitzer MI, Monreal CM, Mayer P (2009) Chemical composition of acid–base fractions separated from bio-oil derived by fast pyrolysis of chicken manure. Bioresour Technol 100:6524–6532

Demirbas E, Kobya M, Konukman AES (2008) Error analysis of equilibrium studies for the almond shell activated carbon adsorption of Cr(VI) from aqueous solutions. J Hazard Mater 154:787–794

Downie A, Klatt P, Downie R, and Munroe P (2007) Slow pyrolysis: Australian demonstration plant successful on multifeedstocks. In: Bioenergy 2007 conference, Jyvaskyla

Erto A, Andreozzi R, Lancia A, Musmarra D (2010) Factors affecting the adsorption of trichloroethylene onto activated carbons. Appl Surf Sci 256:5237–5242

Gaskin JW, Steiner C, Harris K, Das C, Bibens B (2008) Effect of low temperature pyrolysis conditions on biochar for agricultural use. Transactions of the ASABE 51:2061–2069

Gupta VK, Al Hayat M, Singh AK, Pal MK (2009) Nano level detection of Cd(II) using poly(vinyl chloride) based membranes of Schiff bases. Anal Chim Acta 634:36–43

Hameed BH, Tan IAW, Ahmad AL (2008) Optimization of basic dye removal by oil palm fibre-based activated carbon using response surface methodology. J Hazard Mater 158:324–332

Houben D, Evrard L, Sonnet P (2013) Beneficial effects of biochar application to contaminated soils on the bioavailability of Cd, Pb and Zn and the biomass production of rapeseed (Brassica napus L.). Biomass and Energy 57:196–204

Inyang M, Gao B, Yao Y, Xue Y, Zimmerman AR, Pullammanappallil P, Cao X (2012) Removal of heavy metals from aqueous solution by biochars derived from anaerobically digested biomass. Bioresour Technol 110:50–56

Keiluweit M, Nico PS, Johnson MG, Kleber M (2010) Dynamic molecular structure of plant biomass-derived black carbon (biochar). Environ Sci Technol 44:1247–1253

Khan S, Chao C, Arp HPH, Zhu YG (2013) Sewage sludge biochar influence upon rice (*Oryza sativa* L.) yield, metal bioaccumulation and greenhouse gas Emissions from acidic paddy soil. Environ Sci Technol 47:8624–8632

Khan S, Reid BJ, Li G, Zhu YG (2014) Application of biochar to soil reduces cancer risk via rice consumption: a case study in Miaoqian village, Longyan, China. Environ Int 68:154–161

Korea Rural Economic Institute (KREI) (2014) Domestic biomass utilization and revitalization. Seoul

Lu H, Zhang W, Yang Y, Huang X, Wang S, Qui R (2012) Relative distribution of Pb^{2+} sorption mechanisms by sludge-derived biochar. Water Res 46:854–862

Novak JM, Lima I, Xing B, Gaskin JW, Steiner C, Das KC, Ahmedna M, Rehrah D, Watts DW, Busscher WJ, Schomberg H (2009) Characterization of designer biochar produced at different temperature and their effects on a loamy sand. Ann Environ Sci 3:195–206

Rajapaksha AU, Vithanage M, Zhang M, Ahmad M, Dinesh M, Chang SX, Ok YS (2014) Pyrolysis condition affected sulfamethazine sorption by tea waste biochars. Bioresour Technol 166:303–308

Scheckel KG, Ryan JA (2002) Effects of aging and pH on dissolution kinetics and stability of chloropyromorphite. Environ Sci Technol 36:2198–2204

Shinogi Y (2004) Nutrient leaching from carbon products of sludge. In: ASAE/CSAE Annual International Meeting, Paper No. 044063, Ottawa

Smider B, Singh B (2014) Agronomic performance of a high ash biochar in two contrasting soils. Agric Ecosyst Environ 191:99–107

Tan IAW, Ahmad AL, Hameed BH (2008) Preparation of activated carbon from coconut husk: optimization study on removal of 2,4,6-trichlorophenol using response surface methodology. J Hazard Mater 153:709–717

Uchimiya M, Lima IM, Klasson KT, Chang SC, Wartelle LH, Rodgers JE (2010) Immobilization of heavy metal ions (CuII, CdII, NiII, and PbII) by broiler litter derived biochars in water and soil. J Agric Food Chem 58:5538–5544

Uchimiya M, Chang S, Klasson KT (2011) Screening biochars for heavy metal retention in soil: role of oxygen functional groups. J Hazard Mater 190:432–441

Waqas M, Li G, Khan S, Shamshad I, Reid BJ, Qamar Z, Chao C (2015) Application of sewage sludge and sewage sludge biochar to reduce polycyclic aromatic hydrocarbons (PAH) and potentially toxic elements (PTE) accumulation in tomato. Environ Sci Pollut Res. doi:10.1007/s11356-015-4432-8

Xu X, Gao X, Zhao L, Wang H, Yu H, Gao B (2013) Removal of Cu, Zn, and Cd from aqueous solutions by the dairy manure-derived biochar. Environ Sci Pollut Res 20:358–368

Yuan JH, Xu RK, Zhang H (2011) The forms of alkalis the biochar produced from crop residues at different temperatures. Bioresour Technol 102:3488–3497

Zhang P, Ryan JA (1999) Transformation of Pb(II) from cerrusite to chloropyromorphite in the presence of hydroxyapatite under varying conditions of pH. Environ Sci Technol 33:625–630